Meccanica
DOI 10.1007/s11012-014-9915-z

EXPERIMENTAL SOLID MECHANICS

Optimisation and analysis of the reinforcement effect of carbon nanotubes in a typical matrix system

Giorgos Gkikas · Alkiviadis S. Paipetis

Received: 4 October 2013 / Accepted: 19 February 2014

Abstract The scope of this work is the analysis of the reinforcement effect of carbon nanotubes in typical matrix systems, such as epoxy resins. As is well known, efficient dispersion is critical in achieving adequate reinforcement. However, dispersion processes are also well known to degrade the nano-phase. Degradation is manifested as reduction in the aspect ratio as the nanotubes de-agglomerate and break at the same time. For the purpose of this study, multi-wall carbon nanotubes (MWCNTs) with typical length of 1 μm and diameter of 10–15 nm were used for manufacturing MWCNTs/epoxy nano-composites. The inclusion content was 0.5 and 1 % w/w respectively, and dispersion was performed using a typical sonicator gun. The tensile and the fracture toughness properties of the specimens were initially assessed and subsequently optimized. The optimisation process resulted in spectacular improvement in toughness properties. Finally, the antagonistic mechanisms that govern the reinforcement efficient were analysed via the application of the Halpin–Tsai equations for the tensile properties and the distinct contributions of the mechanisms that dissipate energy and enhance toughness, such as the nanotube pull-out, the plastic void growth of the epoxy and the nanotube debonding energy. The de-agglomeration and the aspect ratio reduction were shown to adversely affect the nano-composite properties and create an optimization envelop, well predicted by the employed simple models.

Keywords Carbon nanotubes · Epoxy · Dispersion · Nanocomposites · Toughness · Modeling

1 Introduction

Thermosetting polymers such as epoxies are widely used in the composite material technology and adhesive applications due to their relative high modulus and strength and the high thermal and chemical resistance they present. The curing process of such epoxies results in an amorphous and very high cross-linked network microstructure. This type of microstructure has many useful properties for structural engineering applications. On the other hand, this high cross-linking leads to a very brittle final material with low resistance to crack initiation and crack propagation. Therefore, the incorporation of a second micro- or even nano-structured phase for improving the toughness of such epoxies is required, provided that this type of modification will not affect the other useful properties of the matrix.

Many types of nano-particles have been used to toughen epoxy resins including rubber particles [1–3],

G. Gkikas · A. S. Paipetis (✉)
Department of Materials Science and Engineering, University of Ioannina, Ioannina, Greece
e-mail: paipetis@cc.uoi.gr

Published online: 11 March 2014

thermoplastic particles [4], inorganic particles [5]. In the recent years the nano-modification of the epoxy resins to improve their mechanical and toughness properties has become a standard method involving silica nano-particles [6–8], nanoclays [9–11], carbon nanotubes [12–17], carbon nano-fibers [18, 19] and nano-graphene [20, 21].

Since carbon nanotubes were discovered [22], they have been employed in a variety of applications such as nano-electronics [23], hydrogen storage, nano-devices [24], etc. During the past decade, carbon nanotubes and nano-fibers have been in the forefront of material research as filler material to epoxies for the production of high performance composite structures, extending from aerospace [25] to cultural heritage applications [26], both for structural enhancement and multifunctionality [27–35]. In this direction, the excellent mechanical properties of carbon nanotubes and their high aspect ratio [36, 37] as well as the good interface with polymeric matrices when they are used as reinforcement [38, 39], render them a strong candidate material to achieve reinforcement at the nanoscale. However, it is doubtful that their full potential as reinforcing material can be easily achieved, as their incorporation in the matrix involves a series of technical challenges which often act in an antagonistic way. For example, CNTs have huge surface area and as a result are perfect for instigating all the mechanisms at the interface which form the basis of the remarkable properties of composites. This very surface area is by definition the reason of the agglomeration they are exhibiting. These agglomerates may even act more like a defect of a higher order of magnitude rather than reinforcement at the nanoscale. It is also important to consider that the nano-reinforcement also intervenes in the epoxy network causing adverse behavior during the curing process [40]. Pristine CNTs tend to re-agglomerate during the curing process of the epoxy matrix. Their dispersability is known to be an unstable process, especially at elevated temperatures. The chemistry of the system as well as physical parameters such as temperature and viscosity are responsible for the stabilization of the dispersed CNTs in the epoxy matrix [41]. It was found that chemical functionalization of their surface results in enhanced wettability with the epoxy resin. The attachment of functional groups on their surface prevents re-agglomeration by wrapping them with polymer chains. According to this process, re-agglomeration can be avoided at elevated temperatures, producing composites with uniformly dispersed CNTs [42].

Nonetheless, the introduction of nanotubes in epoxy matrices has often been reported to increase significantly the Young's modulus and the tensile strength of the final material [43–45], as well as its fracture toughness [13, 44, 46]. Also, a reduction of the crack propagation under cyclic fatigue loading, was reported due to the introduction of well dispersed CNTs in polymer matrices [47, 48]. Undoubtedly, efficient dispersion is the key issue to the attainment of properties, such as would be expected by the properties of the nano-graphitic reinforcement [46]. As should be noted, typical homogenization methods which describe the behavior of nano reinforced systems do not account for dispersion effects, although complicated phenomena such as nonlinearities due to fibre-fibre interactions may be included in the model [49].

The energy absorption capabilities of nano-modified epoxy resins is substantially enhanced by the pull-out of CNTs from the epoxy polymer which follows the opening of the faces of the crack during its propagation [46, 50]. This mechanism is potentially the most important one for the increase in the fracture toughness of the nano-composites [51]. At the same time, the CNT pull-out process cannot be initiated if it is not preceded by their detachment from the epoxy matrix, which is a mechanism that also absorbs energy. Successive to the aforementioned mechanisms, is the local reduction of the matrix volume fraction and the possible appearance and development of plastic voids.

The aim of this work is to study the behavior of multi-wall carbon nano-tubes reinforced epoxy polymer in terms of their tensile and fracture toughness properties. To this end, sonication was chosen as the method to disperse the nano-particles to the epoxy matrix. As is known, if the sonication treatment is too aggressive and/or too long, CNTs can be severely damaged, especially when a probe sonicator is employed, suggesting the generation of defects on CNT surface [52]. In extreme cases, the graphene layers of CNTs are completely destroyed and the nanotubes are converted into amorphous carbon [53]. Localized damage of CNTs deteriorates both the electrical and mechanical properties of the CNT/polymer composites. For these reasons, this investigation was focused on how the introduction of nano-

fillers affects the Young's modulus, the tensile strength and the fracture energy of the studied systems in the presence of mechanisms that adversely affect reinforcement, i.e. de-agglomeration and length reduction caused simultaneously by sonication. Two typical CNT loadings were employed, i.e. 0.5 and 1.0 % w/w ratio and for comparison purposes the properties of neat epoxy matrix were also investigated. In order to optimize the input sonication power of the process and simultaneously protect the nano-inclusions from deterioration due to the dissipated energy, an optimization stage was chosen, based on the total energy input required to disperse the nanotubes. Via the introduction of simple models, the contribution of both CNT de-agglomeration and breakage were included in the calculation of the final composite properties. Furthermore, the relative contributions of the pull-out, debonding and void growth mechanisms to the toughness energy were quantitatively modeled. Under the assumption that both de-agglomeration and breakage occur simultaneously, indicative values for tensile modulus, strength and toughness were calculated.

2 Experimental

2.1 Materials

MWCNTs supplied by ARKEMA, France were used as reinforcement in this study. The tube diameter ranged from 10 to 15 nm, the tube length was ranged from 500 nm to 1 μm and the production method was Catalyzed Chemical Vapor Deposition (CVD). A two part low viscosity epoxy resin, i.e. Araldite LY 564 and Aradur 2954, supplied by Huntsman Advanced Materials, Switzerland at a mix ratio of 100:35 by weight was used as matrix material.

2.2 Specimen preparation

An ultrasonic mixer (UP400S, Hielscher, 400 W power, ultrasonic frequency 24 kHz) was used to disperse the CNTs into the epoxy resin. CNTs and Araldite LY 564 resin were carefully weighed and mixed together in a beaker. The total weight of both constituents prepared for sonication was kept at 200gr, corresponding to approximately 220 ml. A 22 mm titanium ultrasonic probe (Sonotrode H22) was

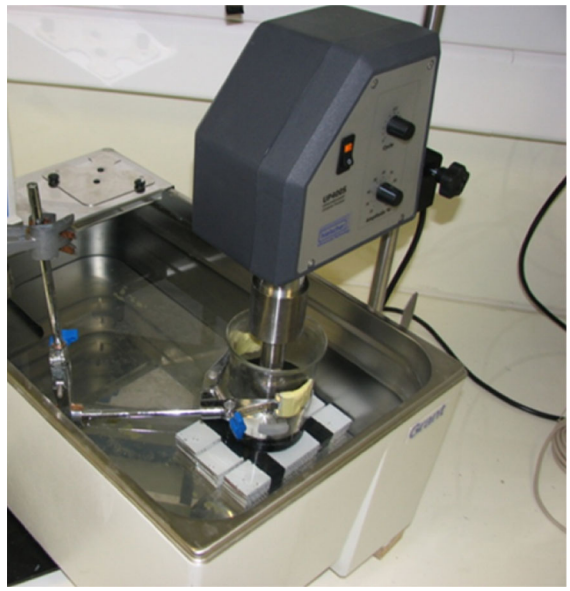

Fig. 1 Sonication process

employed for the mixing process. In order to avoid overheating of the mixture [52], the temperature of the mixture was kept low by submerging the container in a controlled temperature bath (Grant) containing 50 % H_2O and 50 % Ethylene Glycol kept at 5 °C, as shown in Fig. 1.

Two CNT contents (i.e. 0.5 and 1 w/w %) were studied. Initially, the following sonication protocols were used (i) initial stage: sonication for 1 h at full power of the sonotrode was chosen, corresponding to a total energy input of approximately 1.44 MJ, (ii) optimization stage: sonication for 2 h at 50 % amplitude corresponding again to a total energy input of approximately 1.44 MJ. As should be mentioned at this stage, the chosen sonication protocols were designed after an extensive optimization process which involved several protocols [13]. After the sonication was complete, the hardener was added to the modified resin and mixed using a mechanical agitator for about 10 min. To remove entrapped air and voids induced during mixing [54], the mixture was degassed in vacuum oven for 10 min. Finally, the mixture was transferred to silicon rubber molds and cured for 2 h at 60 °C. All specimens were post-cured at 120 °C for 4 h. The specimens for the tensile tests were taken directly from the molds. Their surfaces were grinded and polished before the testing to remove any defect induced by the manufacturing process. The

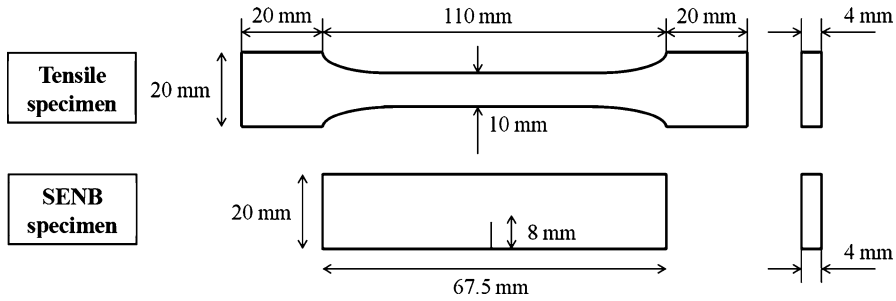

Fig. 2 Specimens configuration and dimensions

specimens used for Single Edge Notch 3-Point Bending tests were cut from a plate and their surfaces were again grinded and polished. The dimensions of the specimens are shown in Fig. 2. At this stage both tensile and SENB tests were performed. At the optimisation stage that followed, only SENB tests were performed, as the main target was to optimize the fracture toughness of the epoxy, which is the most important aspect in the CNT modified epoxy to be employed as a matrix for advanced composites [29, 30, 55].

2.3 Testing procedure

2.3.1 Tensile tests

Tensile tests were performed to evaluate the mechanical performance of the unmodified and modified systems. The tests were performed according to ASTM 638-03 [56].

The specimens were loaded to failure in displacement control mode at a crosshead speed of 0.5 mm/min (corresponding to a strain rate of app. 80 $\mu s - 1$). A video extensometer was used to measure the axial strain of the specimens. Their Young's modulus was calculated from the slope of the stress versus strain curve at the initial stage and the maximum tensile strength calculated from the maximum value of the load. For all configurations five specimens were tested.

2.3.2 Single edge notch 3-point bending (SENB)

The toughness properties of the composites were examined using notched prismatic specimens in single edge notch 3-point bending configuration. Tests were performed according to ASTM D 5045-99 [57].

A 3 mm notch was generated mechanically and a natural crack was created by tapping on a razor blade placed in the notch. The crosshead speed was 10 mm/min.

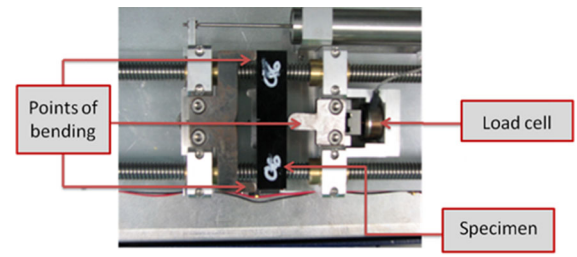

Fig. 3 SENB experimental setup

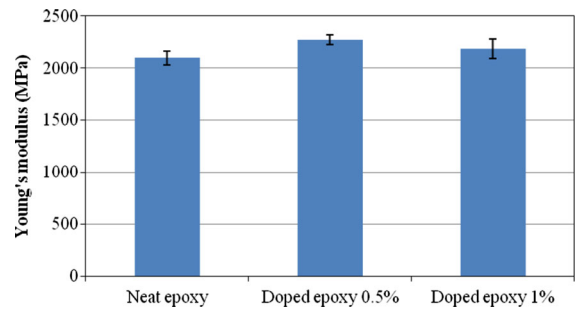

Fig. 4 Young's modulus of the neat epoxy and nanocomposites

The fracture energy of the tested specimens was calculated using the energy method. Five specimens were tested for every one of the configurations. The experimental configuration is shown in Fig. 3.

3 Results and discussion

3.1 Tensile properties

Figures 4 and 5 depict the Young's modulus and tensile strength of the tested specimens which were manufactured at the initial sonication stage. As can be seen in Fig. 4, an improvement of the Young's modulus is documented for both 0.5 and 1.0 % CNT contents compared to the properties of the neat epoxy.

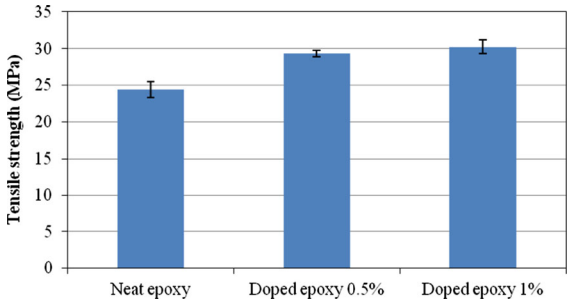

Fig. 5 Tensile strength of the neat epoxy and nanocomposites

Typical of the experimental behaviour of nano-modified systems, is the fact that the tensile modulus deteriorates with the increase in CNT content, implying that the behaviour of the system is nonlinear, or that the reinforcement is limited by the loading of the nano-phase. This effect is readily explained by the assumption that de-agglomeration potential is restricted with increasing CNT content, and therefore reinforcement is inhibited.

It should be noted though that the system with content 1 % w/w CNTs is the one with the highest variation in values between the different specimens tested. The lack of marginal improvement in stiffness with a small addition of carbon nanotubes has been reported [58, 59]. Theoretically, the reinforcement effect from the CNTs to the epoxy resin is attributed to the effective load transfer from the matrix to the CNTs. Consequently, the optimal dispersion of the nano-fillers to the matrix has to be achieved. However, the larger the provided interface, the more difficult it is to efficiently disperse the reinforcing phase [60].

The tensile strength of the specimens exhibited an enhancement for the modified systems compared to the neat resin. The conditions for the chosen sonication process are in good agreement with previous work published on the effect of the sonication on the mechanical properties of CNT modified epoxy systems, where it was shown that improvement was achieved when sonication time varied between 1 and 2 h [61]. Notably enough, the CNT content increase from 0.5 to 1.0 % did not affect the maximum value, as the results for the modified systems are well within the experimental scatter. Unlike in the case of stiffness, the system with 1 % retains the improved strength, which indirectly implies that the CNTs affect more the properties that are less related to the linear elastic behaviour of the composite.

3.2 Fracture properties

In view of the above, the incorporation of CNTs may favour more properties which are more related to the damage tolerance of the nano-composite or its resistance to crack initiation and propagation [29], rather than properties related to its elastic behaviour. The mechanisms that could justify this enhancement relate to crack deflection and bifurcation mechanisms which are instigated by the presence of the nano-phase, which involve failure at the nano-scale. These effects may also indirectly affect the viscoelastic properties of the nano-composites, as the scale of the damage initiation and propagation is of the same order of magnitude of the polymer microstructure [13, 25].

The requirement for maximum improvement in properties is directly dependent on maximum de-agglomeration and minimum damage of the CNTs, which occur simultaneously during dispersion. It can be safely postulated that these two mechanisms: (i) are interdependent and (ii) possess an energy influx threshold above which they are triggered. Obviously, de-agglomeration favours reinforcement and CNT breakage inhibits reinforcement. Being extremely stiff and nano-scaled, CNTs required high energy influx to break, and as a result, it may be assumed that the energy required for the de-agglomeration of the CNTs is lower than that required for the CNT breakage. This postulation can also be based on the fact that CNT strength is a length dependent property [62], as is typically the case for carbon fibres [63, 64]. In this case, even if de-agglomeration involves CNT breakage, as CNT length is reduced their respective strength is enhanced and therefore the energy density required to break them is increasing. In other words, the optimisation of the properties of the nano-composite may be achieved via the modification of the sonication power input for total input energies that indicate property improvement, as indicated by the power time product. Such an optimisation would involve the examination of the optimal total energy throughput, as well as the examination of different power inputs for protocols that yielded the best fracture properties.

To this end, the dispersion protocol applied for both CNT contents involved sonication for 2 h at 50 % amplitude. In other words, the energy input in the system was kept constant but the power was reduced to half to favour CNT de-agglomeration to CNT breakage. This protocol aimed at defining the optimisation

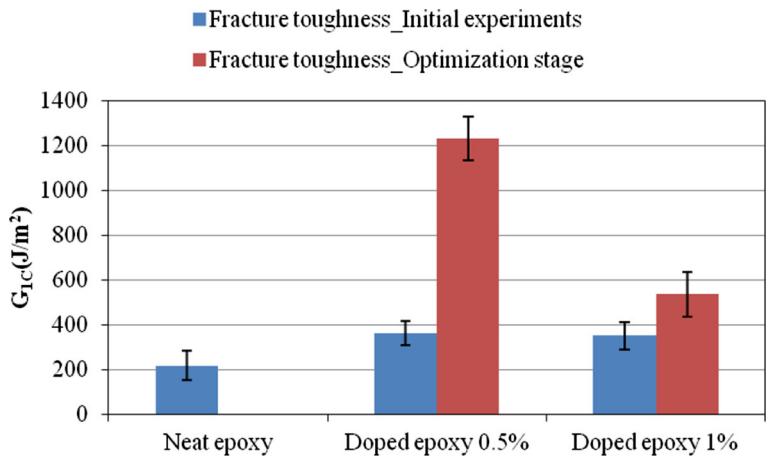

Fig. 6 Fracture toughness of the neat epoxy and nano-composites

window for the maximum fracture toughness of the CNT-epoxy nano-composites, as was successfully performed in a previous study [13].

Figure 6 depicts the fracture toughness of the tested materials during the two stages, the initial and the optimisation stage. As can be seen, for the initial experiments there is an enhancement of the fracture toughness for both the doped systems. In the case of the 0.5 %, the increase in fracture toughness is spectacular reaching almost 400 % compared to the initial sonication protocol and almost 600 % compared to the neat epoxy system. The 1.0 % CNT nanocomposite exhibits significant but much less spectacular enhancement, with 50 % enhancement compared to the initial sonication protocol and 130 % enhancement compared to the neat epoxy. This directly related to the effect that was observed in the case of the tensile properties, where the increase in CNT content does not improve or even deteriorate the composite properties. The increase in CNT content requires higher power to successfully de-agglomerate the nanoparticles which in turn would favour damage and breakage of the CNTs. This finding strongly suggests that the dispersion effect on the reinforcing ability for nano-composites systems are highly non-linear in that they possess a CNT loading threshold above which the degradation mechanism is favoured to the de-agglomeration mechanism and therefore becomes dominant for higher CNT contents.

Recapitulating the experimental findings, the dispersion process possesses an impressive optimization window for improving toughness properties. At the same time, the postulations that (i) different CNT dispersion mechanisms in epoxy are triggered at different powers and (ii) dispersion may be optimized when only ''favourable'' dispersion mechanisms are active which may be saturated (or optimized) at a given energy input where also verified as the higher CNT content exhibited less enhancement during the optimisation stage.

3.3 Modeling studies

The experimental campaign that preceded this section revealed that there are distinct antagonistic mechanisms during dispersion that govern the reinforcing ability of the nano-phase. In order to approach theoretically this behavior, the assumption that two mechanisms are simultaneously taking place with constant volume fraction may be performed:

1. Dispersion of the agglomerates: The reinforcement consists of cylindrical agglomerates with constant length which reduce in radius from a multiple of the original CNT diameter D_f to $1D_f$ with the sonication process
2. Reduction of the aspect ratio of CNTs: The reinforcement consists of well dispersed CNTs that break with the sonication process, which would reduce the original length L_f to a fraction of it.

Figures 7 and 8 depict the aforementioned principles. (i) the reinforcing particle is of cylindrical shape where the height of the cylinder ranges from the initial nanotube length L_f to a fraction of it ($L_f/20$) and (ii) the diameter of the cylinder ranges from the nominal reinforcement diameter D_f to a multiple of it ($20\ D_f$), while the total volume fraction of the reinforcement is kept constant. The dispersion process involves both

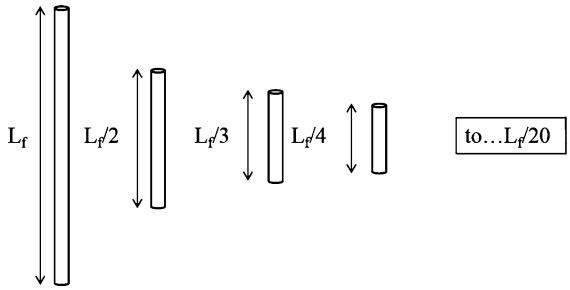

Fig. 7 Representation of the assumption of the length reduction of the CNTs

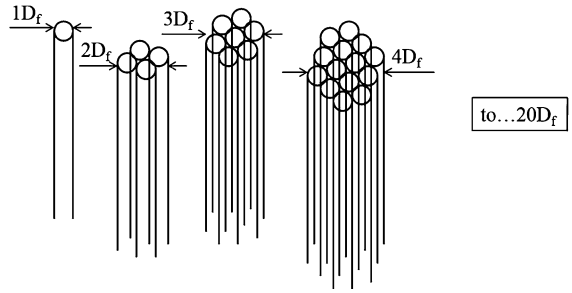

Fig. 8 Representation of the assumption of the agglomeration of the CNTs

the length reduction of the CNTs from their original length L_f to $L_f/20$ and the de-agglomeration process involves the de-agglomeration of the CNT bundles from 20 to 1 D_f where the single CNT possesses a diameter D_f and constant length L_f. If these processes occur simultaneously, the common solution of the composite properties for both mechanisms using any homogenized model will provide the equivalent properties of the nano-reinforced composite. Favoring any of the two mechanisms will provide the optimisation (or degradation) envelop that delineates the process dependent properties of the composite.

In view of the above, the effect of the CNT length to the respective property of the final material was studied by reducing their length from 1 to 20 times. The average length of the carbon nanotubes employed for the initial calculation was the mean value provided by the manufacturer (i.e. 750 nm) while the minimum (500 nm) and the maximum (1 μm) were used for the minimum and maximum standard deviation of the results. Furthermore, the effect of the size of the agglomeration was investigated. According to the above hypothesis, we assumed effects from 1 single nanotube (with diameter 15 nm) to agglomerations with diameter 20 times the diameter of the single nanotube. The average carbon nanotube's diameter was used for the calculations while the minimum and maximum length was used again for the standard deviation of the results. In the following modeling studies, two different CNT contents were assumed, i.e. 0.5 and 1 %. The MWCNT density has been estimated to be on average 1.65 g/ml [65], by assuming a tubular structure of graphene planes, where the outer diameter is twice the inner. However, if the voids near the crossings between MWNTs (i.e. the spaces that cannot be filled by other MWNTs) are accounted for, the density is considerably reduced to 1.30 g/ml, as reported via Scanning Electron Microscopy studies [66]. This value is close to the density of the employed matrix, i.e. 1.2 g/ml, as quoted by the manufacturer. Therefore, for reason of simplicity, the density of the matrix and the reinforcing nano-phase were assumed to be equal for the purposes of this study, i.e. the weight fraction of the reinforcement is assumed to coincide with the volume fraction.

The next step of this work involves the adoption of appropriate analytical models in order to adequately describe the Young's modulus, the tensile strength and the fracture toughness of the modified nanocomposites, as a function of the CNT length and the agglomerate diameter.

3.3.1 Young's modulus

The following analysis is based on the model proposed by Yeh et al. [66]. Their model is based on the Halpin–Tsai approach to describe the unidirectional fiber reinforced composites properties based on the improvement of the simple rule of mixtures to account for shape and aspect ratio of the reinforcement [67]. According to this model the composite Young's modulus E is given:

$$E = \frac{1 + \xi\eta V_f}{1 - \eta V_f} E_m \tag{1}$$

where V_f is the volume fraction of the nano-reinforcement, E_m is the Young's modulus of the neat matrix, ξ is a shape factor related to the aspect ratio of the reinforcement given by:

$$\xi = 2\left[\frac{l_f}{D_f}\right] \tag{2}$$

L_f and D_f are the length and the diameter of the inclusion respectively and η is a parameter given by:

$$\eta = \frac{\left[\frac{E_f}{E_m}\right] - 1}{\left[\frac{E_f}{E_m}\right] + \xi} \tag{3}$$

in which E_f is the Young's modulus of the reinforcement.

The Halpin–Tsai equation was originally used for fibrous composite materials with aligned reinforcement. In the case of randomly dispersed nano-materials the model has to be modified to account for waviness or the random distribution on the properties of CNT-modified epoxies [68–70]. The orientation factor k was introduced by Cox into the Halpin–Tsai equation by modifying the value of the aspect ratio parameter, ξ in order to account for randomly oriented fibres in the composite [71]. k accounts both for the randomness of the discontinuous fibers and the relationship between the thickness of the specimen and the length of the reinforcement. In other words it describes the difference between the two dimensional and the three dimensional dispersion of the nanoreinforcement in the matrix. Hence, when the fiber length is smaller than the thickness of the specimen, the parameter $k = 1/6$ is used for the Young's modulus of the material. On the other hand, when the length of the reinforcement is longer than the thickness of the specimen, $k = 1/3$ [71]. In our study the specimen thickness was 4 mm while the length of the reinforcement varied from 500 nm to 1 μm. In this respect, it may be assumed that since the reinforcement is considerably smaller than the thickness of the specimen, the dispersion is three dimensional, which is arguable the case for all nano-scaled fillers. Therefore $k = 1/6$ was employed for this study.

Consequently the Eq. 3 is transformed as following:

$$\eta = \frac{\left[\frac{kE_f}{E_m}\right] - 1}{\left[\frac{kE_f}{E_m}\right] + \xi} \tag{4}$$

In Eqs. 1–4 the only unknown value is E_f. The length and the diameter of the reinforcement (l_f and D_f), are provided by the manufacturer of the CNTs, the volume fraction (V_f), of the inclusion is defined by the experimental protocol and the Young's modulus of the matrix was calculated experimentally and its value was in good agreement with the value provided by the manufacturer (datasheet). According to the literature [72], a good estimation for the Young's modulus of the reinforcement is 1,100 GPa. This is in good agreement with other sources where the tensile modulus of MWCNTs was estimated at 953 GPa [73] or to at in range of 250–1,200 GPa [74]. In our work the Young's modulus of the reinforcement used was selected to be 1,000 GPa. It should be noted that the difference over the full modulus range results in less than 5 % variation in the maximum value of the calculated composite stiffness.

As aforementioned, the Young's modulus of the nano-composite is not increased in a linear way with the addition of higher loading of nano-reinforcement, but may even be reduced at higher volume fractions due to the agglomerations. To account for this effect, the ξ parameter related to the aspect ratio of the reinforcement was further modified, Eq. 5, introducing an exponential factor to account the effect of the agglomeration to the stiffness of the final material [66, 75].

$$\xi = 2\left[\frac{l_f}{D_f}\right] e^{-\alpha V_f - b} \tag{5}$$

In this representation of ξ, α and b are constants related to the degree of the CNTs agglomeration. According to Yeh et al. [66], for a phenolic polymer modified with two types of MWCNTs, two values of the parameters were calculated, 75 and 55 for the parameter α and 1.0 and 0.5 for the parameter b. The higher values represent MWCNTs arranged in a network while the lower values represent MWCNTs randomly dispersed. According to another approach [72], parameter α was calculated 9.15 while parameter b was calculated 0.12. The lower values for the parameters in the last approach indicate better dispersion of the nano-fillers. In our study the mean value was selected, i.e. the value 55 for the parameter α and the value 0.5 for the parameter b because of the randomly dispersion of the reinforcement. Again, the sensitivity study on the range of a values revealed less than 1 % variation in the variation in the maximum value of the calculated composite stiffness.

The results for the Young's modulus of the nano-composites are shown in Figs. 9 and 10 below. In this figures, the dispersion process is following the reduction of both the agglomerate diameter and the CNT length. With the assumption the both mechanisms occur simultaneously, the common solution of the two functions corresponds to a value of 2.17 GPa for 0.5 %

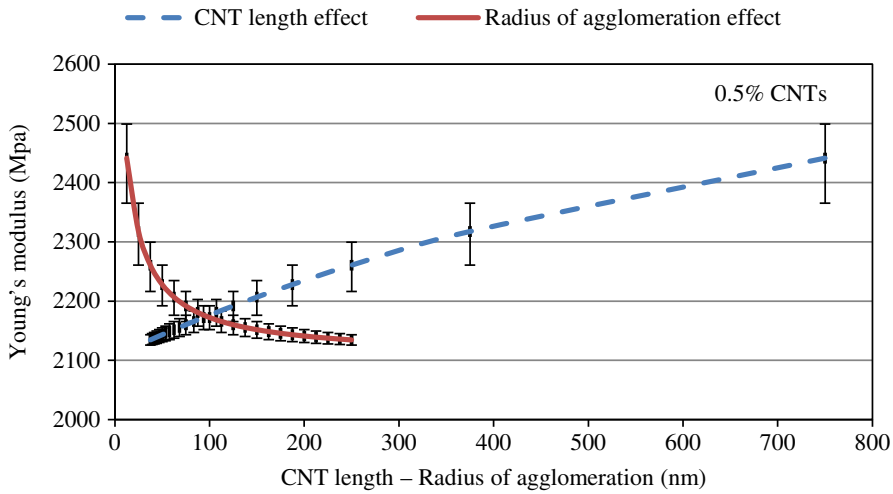

Fig. 9 The effect of length reduction and agglomeration to the Young's modulus of modified epoxy with 0.5 % w/w CNTs

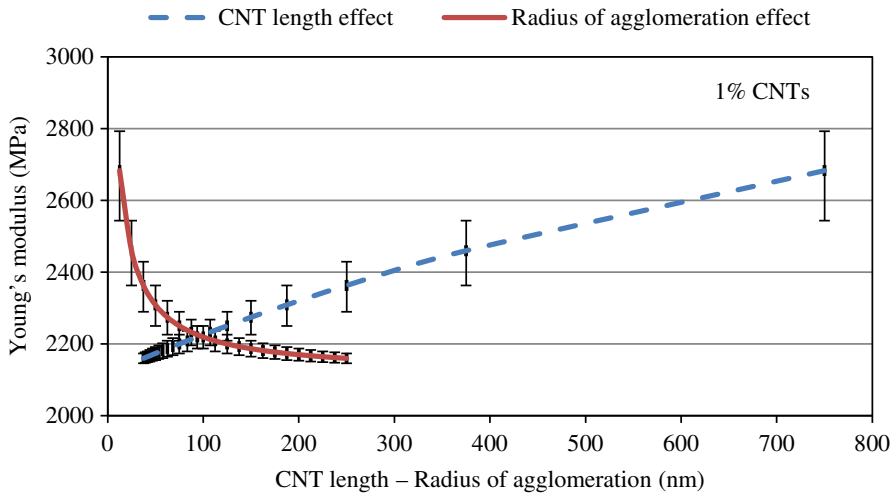

Fig. 10 The effect of length reduction and agglomeration to the Young's modulus of modified epoxy with 1 % w/w CNTs

and 2.22 GPa for 1 %. According to the adopted approach, any value above the calculated one denotes that de-agglomeration prevails to the nano-reinforcement breakage. On the contrary, any value below the calculated one denotes either that the dispersion is not efficient, or that the length of the nano-reinforcement is substantially reduced.

For 0.5 % CNTs, the experimentally defined value for the Young's modulus was 2.27 ± 0.05 GPa (Fig. 4), which compare well with the predicted values from the Halpin–Tsai model. According to the adopted approach, the experimentally achieved value is above the common solution of 2.17 GPa, suggesting that the employed dispersion protocol yielded satisfactory values by favoring de-agglomeration to breakage. On the contrary, the common solution corresponding to the two antagonistic mechanisms for 1.0 % is 2.22 GPa as compared to an experimental value of 2.18 ± 0.09 GPa, indicating either that the dispersion protocol does not suffice to break the agglomerates or that the nano-reinforcement is damaged via the dispersion process. This is in good agreement with previous studies [60], where it was observed that as the CNT content increases, the larger the provided interface, and consecutively the more difficult it is to efficiently disperse the reinforcing phase. In both cases, if the size of the agglomeration is too big or the length of the nanotubes is reduced very

much the results for the Young's modulus come closer to that of the neat epoxy resin.

3.3.2 Tensile strength

For the calculation of the tensile strength of the specimens, the Halpin–Tsai equations were employed similarly to that of the Young's modulus, as reported in the approach by Yeh et al. [66]. As is well known, the Halpin–Tsai equations were formulated for elastic properties and not for strength properties. However, on a theoretical basis, the composite strength follows a "rule of mixtures approach" (i.e. the composite property is the sum of the constituent properties multiplied by their V_f), if both phases of the composite fail at equal strain [76]. This is valid either for low volume fraction if the fibre strain to failure is higher than that of the matrix, or for high volume fractions if the fibre strain to failure is higher than that of the matrix [76]. Typical values for the employed epoxy as given by the manufacturer are 4.5–5.5 %. On the other hand, the strain to failure of MWCNTs is reported to be as high as 12 % [77]. Thus, in the studied case, we are dealing with a "low volume fraction system" where the matrix fails at lower strains than the reinforcement. As aforementioned, in this case the strain to failure of the composite is governed by the strain to failure of the matrix and the rule of mixtures hypothesis is valid for the strength of the constituents [76]. Moreover, in the case of "large volume fractions", the higher failure strain of the reinforcement would result in macroscopic fibre bridging as is typically the case in ceramic matrix composites. However, this would not be plausible both due to the scale and the random orientation of the reinforcement. Indeed, as expected, no bridging effects were noted at the macroscale during the experimental testing.

From Eq. 1, by substituting the tensile modulus with tensile strength values the Halpin–Tsai equation becomes:

$$\sigma = \frac{1 + \xi\eta V_f}{1 - \eta V_f}\sigma_m \tag{6}$$

where V_f is the volume fraction of the nano-reinforcement, σ_m is the tensile strength of the neat matrix, ξ is a shape factor related to the aspect ratio of the reinforcement given by Eq. 2 above and η is a parameter given by Eq. 7 below.

$$\eta = \frac{\left[\frac{\sigma_f}{\sigma_m}\right] - 1}{\left[\frac{\sigma_f}{\sigma_m}\right] + \xi} \tag{7}$$

As discussed in the previous section, Cox [71], modified the parameter η by introducing the parameter k used into the Halpin–Tsai equation by modifying the value of the aspect ratio parameter, ξ:

$$\eta = \frac{\left[\frac{k\sigma_f}{\sigma_m}\right] - 1}{\left[\frac{k\sigma_f}{\sigma_m}\right] + \xi} \tag{8}$$

According to Yeh et al. [66], and as was confirmed by the preceding experimental campaign, nanocomposites exhibit a non-linear behavior by increasing the CNT content, which is similar to the Young's modulus model described previously. Thus the shape factor ξ is transformed according to the Eq. 9 below.

$$\xi = 2\left[\frac{l_f}{D_f}\right] e^{-aV_f - b} \tag{9}$$

According to Yeh et al. [66], for a phenolic polymer modified with two types of MWCNTs, two values of the parameters were calculated, 65 and 40 for the parameter a and 1.1 and 1.0 for the parameter b. The higher values represent MWCNTs arranged in a network while the lower values represent MWCNTs randomly dispersed. It should be noted that for total range of a values, the calculated composite strength varies less than 3 % of its maximum value, i.e. the geometrical properties of the reinforcement are the main variation in the calculated composite strength values. For the calculation of strength, the second solution was selected, i.e. the value 40 for the parameter α and the value 1.0 for the parameter b because of the random dispersion of the reinforcement.

Tensile strength of MWCNTs was found to range between 11 and 63 GPa [73] and in some cases reaches at 150 GPa [78]. In our study the average value of 30 GPa from [73] was employed. The tensile strength of the epoxy matrix was defined from tensile tests of unmodified epoxy specimens. As in the case of a, for the total range of CNT strength values (0.1–1 GPa), the calculated composite strength varies less than 1 % of its maximum value, i.e. again the geometrical properties of the reinforcement are the main variation in the calculated composite strength values.

Following the same approach as for the stiffness, (de-agglomeration vs. breakage) the calculated values

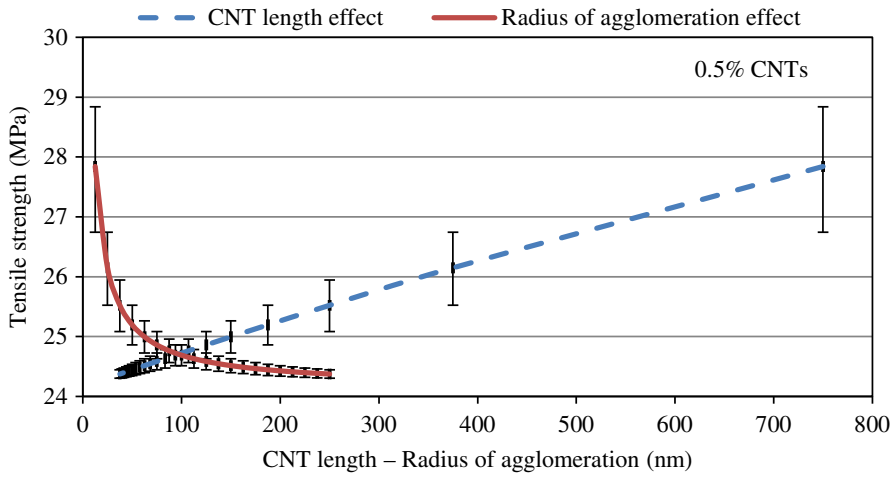

Fig. 11 The effect of length reduction and agglomeration to the tensile strength of modified epoxy with 0.5 % w/w CNTs

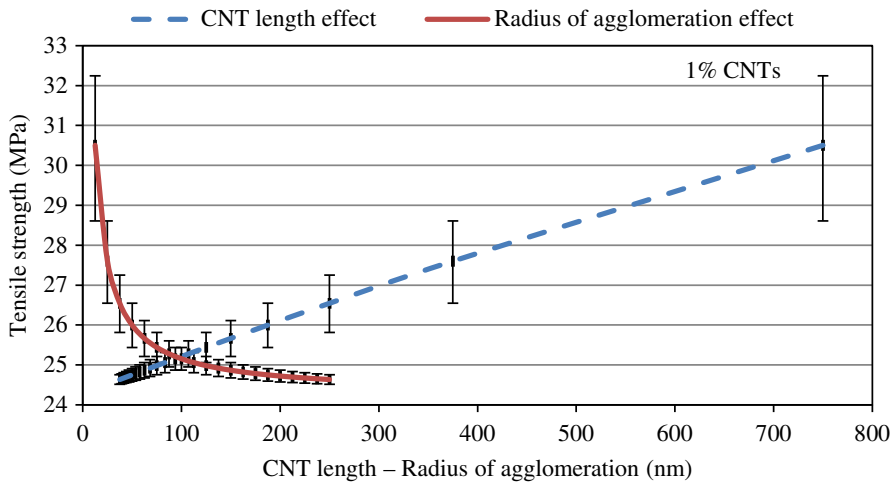

Fig. 12 The effect of length reduction and agglomeration to the tensile strength of modified epoxy with 1 % w/w CNTs

for the tensile strength of the nano-composites are shown in Figs. 11 and 12 below for 0.5 and 1.0 % CNT loading respectively.

The calculated common solution for de-agglomeration and breakage for 0.5 and 1.0 % loading is 24.7 and 25.2 MPa respectively. The experimentally defined values are 29.3 ± 0.4 and 30.2 ± 1.0 MPa for 0.5 and 1.0 % loading respectively. In this case, both systems seem to have attained the maximum possible reinforcement efficiency with the 0.5 % CNT loading exhibiting again higher reinforcement effect than the 1.0 % loading. The attainment of the maximum reinforcement efficiency for both systems as calculated via the modified Halpin–Tsai model indicates either that the composite strength is less sensitive to the dispersion process than the tensile modulus or that the mechanisms that lead to the tensile failure of the nano-reinforced composite require more elaborate analytical description than the modified Halpin–Tsai model since failure in the presence of the nano-phase involves highly non-linear processes related to the creation and propagation of cracks at the nano-scale, as is elaborated in the next section. This may also be attributed to the inherent hypothesis of the model of equal strain to failure for both the matrix and the reinforcement.

3.3.3 Fracture properties

The modeling approach adopted to study the effect of the antagonistic reinforcing mechanisms is described by Hsieh et al. [72]. In order to study the effect of the nano-reinforcement to the toughness of the modified epoxies,

three main toughening mechanisms were assumed to contribute to the final fracture energy: (i) the CNT pull-out energy, (ii) the energy from the debonding of the CNTs from the polymeric matrix and (iii) the energy from the plastic void growth due to the pull-out of the nano-fillers. Fiber pull-out, has been shown to be the main source of energy dissipation and thus toughness in carbon fiber reinforced polymers [46, 79–82].

In the case of MWCNTs, there are two different pull-out mechanisms, i.e. (i) the nanotube pull-out from the epoxy matrix and (ii) the sword-in-sheath mechanism [50]. In the case of the latter mechanism, the outer shell of a MWCNT fractures in tension while the inner shells pulls-out from it. Generally, the pull-out phenomenon increases the toughness of the nano-composites by the interfacial friction between the body of the filler and the surrounding matrix. The surface area of the carbon nanotubes typically ranges between 1,000 and 1,200 m^2/gr [15], which explains the high potential of this mechanism towards the increase of the final fracture energy.

The work due to the shear acting at the interface of a single fibre during an infinitesimal slide dx is:

$$dU = (2\pi r x \tau_{i^*})dx \tag{10}$$

where x is the embedded length of the fiber τ_{i^*} is the interfacial shear stress and dx is the distance of the pull-out.

The total pull-out work for a single fibre is:

$$\Delta U = \int_0^{x_0} 2\pi r x \tau_{i^*} dx = \pi r x_0^2 \tau_{i^*} \tag{11}$$

The pull-out work of fracture G_{cp} for involved fibres in the pull out process is given by:

$$G_{cp} = \int_0^{L} \frac{N dx_0}{L} \pi r x_0^2 \tau_{i^*} \tag{12}$$

The total number of the fibers, N, is related to the fibre volume fraction:

$$N = \frac{V_f}{\pi r^2} \tag{13}$$

Substituting to Eq. 12 and integrating, yields the final expression for the pull-out energy:

$$\Delta G_{pull-out} = \int_0^{l_e} \frac{N dx}{l_e} \pi r_f x^2 \tau_i \tag{14}$$

$$\Delta G_{pull-out} = \frac{V_{fpo} l_e^2 \tau_i}{3 r_f} \tag{15}$$

where l_e is the effective pull-out length of the fiber whose maximum value equals half the nanotube length l_f, r_f is the radius of the fiber or nanotube, x is the length involved in pull-out, τ_i is the interfacial shear strength, N is the number of the nanotubes per unit area, V_f is the volume fraction of the nanotubes and V_{fpo} is the volume fraction of the nanotubes which are pulled-out. It is important to note that the effective pull-out length is not necessarily equal to the total length of the nanotubes, as only a portion of the nanotube is involved in the pull out process, which depends on the interfacial shear strength and the axial strength of the reinforcement. However, in the case of MWCNTs, the condition for the axial strength to overpass the maximum embedded length, or half the mean nanotube length is easily satisfied for lengths less than 1 μm due to the extraordinary strength of the tube, and hence it can be safely assumed that the nanotubes are pulled out from the polymer matrix without failing axially.

Several studies have been performed aiming at the calculation or measurement of the interfacial shear strength of CNTs in polymer matrices. Values reported range from 1 to 100 MPa when strong bonding between the fiber and the matrix is present (i.e. covalent bonding) [50, 83, 84]. According to [83], the interfacial shear strength between carbon nanotube and polymer matrix was calculated to 47 MPa by attaching a single MWCNT to an AFM tip. Similar values are reported for typical carbon fibre epoxy interfaces [29], or CNT modified carbon fibre epoxy interfaces [32], which typically correspond to the adhesion efficiency of oxidized or sized graphene layers on epoxy resin [27]. Consecutively, a value of 47 MPa was chosen for the purposes of this study.

It should be noted that the pull-out process involves the creation of a fracture surface and is not a volume effect, and as a result not all the incorporated nano-fillers are involved in pull-out phenomenon. As is reported by Hsieh et al. [72], the CNT fraction that is involved in the pull-out process depends on the CNT volume fraction and is reduced as the CNT content increasing due to agglomerations. Furthermore, as the nanotubes are long and not straight, they rapture rather than pulling out completely, decreasing the fraction involved in the pull-out process. Based on their

approach, the calculated fractions that are involved in the pull out process are 0.317 for 0.5 % w/w CNT and 0.420 for 1 % w/w CNT.

As has been reported [85], the contribution from the plastic void-growth mechanism to the fracture energy is:

$$\Delta G_V = \left(1 - \frac{\mu_m^2}{3}\right)\left(V_{fv} - V_{fp}\right)\sigma_{yc} r_{yu} K_{vm}^2 \tag{16}$$

where V_{fv} and V_{fp} are the volume fraction of the voids and the volume fraction of the nanotubes, μ_m is the material constant allowing for the pressure-dependency of the yield stress and chosen to be 0.175 [86], K_{vm} is the maximum stress concentration for the von Mises stresses around a debonded particle, which is related to the volume fraction of the reinforcement [87, 88]. The value of K_{vm} was selected to be 2.11 [6, 88]. σ_{yc} is the comprehensive yield stress and according to the datasheet varies between 110 and 140 MPa. A median value (120 MPa) was used for the calculations. The value of $(V_{fv} - V_{fp})$ used for the 0.5 % w/w CNT content was 0.024 %, [72], while for the system with 1 % w/w of CNT content was 0.048 %, as it is reported to vary linearly with volume fraction [72]. Finally, r_{yu} is the plastic zone size at fracture of the unmodified epoxy resin and can be calculated from Eq. 17 below.

$$r_{yu} = \frac{1}{6\pi}\frac{E_m G_{CU}}{(1 - \upsilon^2)\sigma_y^2} \tag{17}$$

where G_{CU} is the fracture energy, v is the Poisson's ratio and σ_y is the tensile yield stress of the unmodified matrix. The Poisson's ratio of the neat epoxy matrix is 0.35 according to the manufacturer's datasheet; the fracture toughness and the tensile yield stress of the neat matrix were measured at 217.7 J/m^2 and 24.0 MPa respectively.

The work done when a single fiber undergoes interfacial debonding can be written as follows, Eq. 18.

$$\Delta U = 2\pi r x_0 G_{ic} \tag{18}$$

where x_0 is the embedded length of the fiber on the side of the crack where debonding occurs ($x_0 \leq l_e = \frac{l_f}{2}$) and G_{ic} is the fracture energy of the interface. Assuming that there are N fibers per m^2, then there are $\frac{N dx_0}{l_e}$ per m^2 with an embedded length between x_0 and $(x_0 + dx_0)$. The total debonding work is given by:

$$\Delta G_{db} = \int_0^{l_e} \frac{N dx_0}{l_e} 2\pi r x_o^2 G_{ic} \tag{19}$$

From Eq. 13, N is related to the fiber volume fraction V_f and the fiber radius r and by substituting to Eq. 19 and integrating the expression of the interfacial debonding energy is yielded [16]:

$$\Delta G_{db} = \frac{V_{fdb} l_f G_{ic}}{2D_f} \tag{20}$$

where V_{fdb} is the volume fraction of the nanotubes which debond and selected to be 0.317 for the 0.5 % w/w of CNT content and 0.420 for the 1 % w/w of CNT content, G_{ic} is the interfacial fracture energy between the CNT and the epoxy matrix. Several results for this parameter have been reported. According to [83, 89], values from 13 to 34 J/m^2 have been exported. Hence a median value of 25 J/m^2 will be used in our study.

By summing all the contributions from the distinct energy dissipation mechanisms as described above, the total fracture energy of the nano-modified epoxy composites is:

$$G_C = G_{CU} + \Delta G_{pull-out} + \Delta G_V + \Delta G_{db} \tag{21}$$

where G_{CU} is the experimentally measured fracture energy of the neat epoxy matrix at 217.7 J/m^2. As should be noted, in the above equation, G_{CU} is constant and ΔG_V depends only on volume fraction. For the studied cases, this yields a base value of 254.5 J/m^2 and 291,3 for the for the 0.5 % and the 1 % volume fraction respectively, where the effect of pull-out and debonding are added to calculate the total energy. In the employed model, the contributions from pull-out and debonding are calculated to be approximately equal.

The values of all parameters used for construction of the model are shown in Table 1 below.

The results for the predicted values are shown in Figs. 13 and 14 below.

In Fig. 13, the effect of the agglomeration and the CNT breakage to the fracture energy for 0.5 % CNT content is depicted. As was performed in the case of modulus and strength, the common solution from the two competing mechanisms yields a value of 369 J/m^2, which is very close to experimentally measured value of 361 ± 52 J/m^2, measured experimentally for the initial sonication protocol. The optimized protocol

Table 1 Values of the parameters used in the modelling studies

Name	Symbol	Unit	Value	Source
Diameter of the nanotube after sonication	D_f	nm	12.5	12.5 or longer assuming agglomerations
Length of the nanotube after sonication	l_f	nm	750	750 or lower assuming length reduction due to process
Young's modulus of nanotubes	E_f	GPa	1,000	[72–74]
Young's modulus of unmodified epoxy	E_m	MPa	2096.69	Present study
Fracture energy of unmodified epoxy	G_{CU}	J/m^2	217.7	Present study
Orientation related constant	k	–	1/6	[71]
Agglomeration related constant	a	–	55	[66]
Agglomeration related constant	b	–	0.5	[66]
Interfacial shear strength	τ_i	MPa	47	[83]
Poisson's ratio for unmodified epoxy	v		0.35	Datasheet
Plane strain comprehensive yield stress of unmodified epoxy	σ_{yc}	MPa	120	Datasheet
Pressure dependent yield stress parameter	μ_m	–	0.175	[88]
Maximum von Mises stress concentration	K_{vm}	–	2.11	[6, 88]
Uniaxial tensile yield stress	σ_y	MPa	24.04	Present study
Interfacial fracture energy	G_i	J/m2	25	[83, 89]

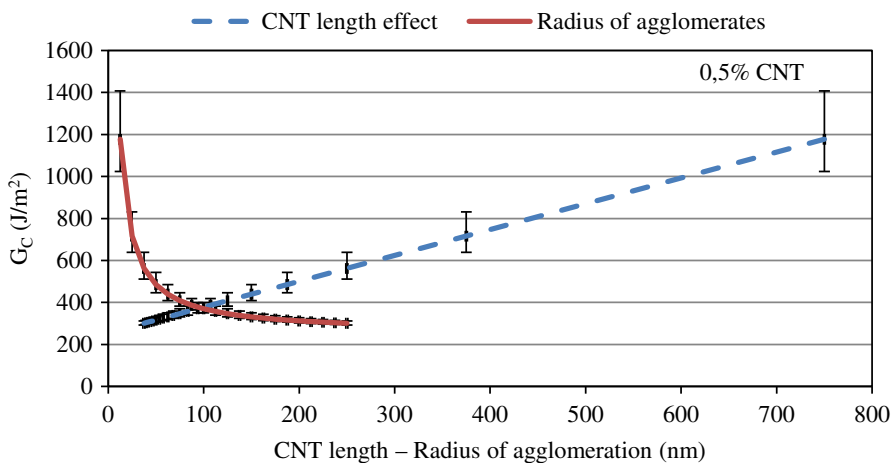

Fig. 13 Fracture energy of the modified epoxy with 0.5 % CNTs assuming agglomeration effect and CNT length reduction because of the sonication procedure

that followed, yielded a value of 1.332 ± 98 J/m^2, which are shifted towards the optimal properties, suggesting clearly that the de-agglomeration process is becoming the dominant mechanism and the nano-composite properties are close to being maximized, although there is still room for improvement.

In the case of 1 % w/w CNT content, the assumption of the common solution yields a value of 445 J/m^2 which is substantially more that the measured value of 351 ± 61 J/m^2. The minimum calculated value assuming an agglomerate of 20 CNTs or equivalently a 20-fold reduction in the CNT length is calculated to be 352 J/m^2, suggesting that the employed sonication protocol barely managed to break the agglomerates to diameters less than 250 nm, which was the limit for the performed calculated values, and practically the value where the energy asymptotically tends (Fig. 14). As was the case for the composite stiffness, the results suggest that the higher concentrations of CNTs inhibit de-agglomeration suggesting again that there may be a CNT loading limit above which the nano-reinforcement may not be dispersed without seriously

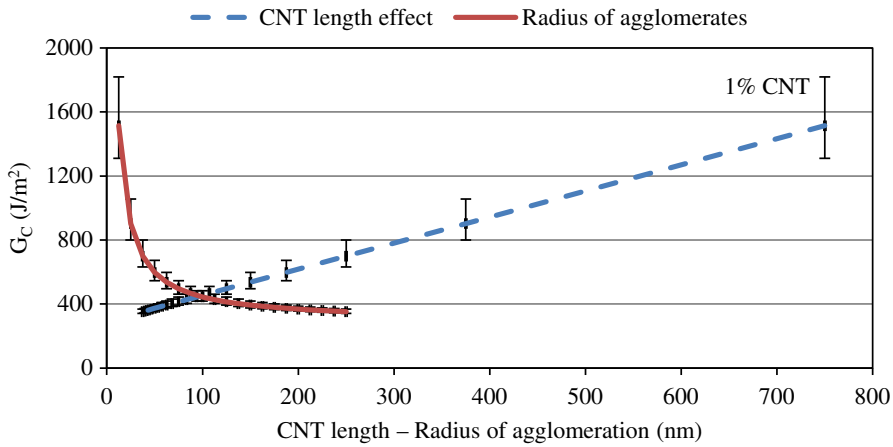

Fig. 14 Fracture energy of the modified epoxy with 1 % CNTs assuming agglomeration effect and CNT length reduction because of the sonication procedure

damaging it and compromising its reinforcing properties. However the application of the optimized protocol yielded a substantial increase in the nanocomposite toughness, albeit not as impressive as in the case of the 0.5 % loading. The attained value of 536 $\pm$ 99 J/m^2, indicates that the applied sonication protocol has successfully favored the de-agglomeration mechanism to the breakage of the nanotubes, suggesting that efficient reinforcement is still feasible at 1.0 % CNT loading.

4 Conclusions

The aim of this work was to study the interrelation between the efficient dispersion of MWCNTs is epoxy matrix with the employed dispersion methodology. Within the scope of the study was the realization of optimisation strategies for the attainment of the maximum reinforcing ability of the nanotubes in conjunction with the identification of the competing mechanisms that govern nanoreinforcement.

The major mechanisms that govern nanoreinforcement were identified to be (i) the de-agglomeration of the CNTs together with the (ii) damage of the CNTs as manifested by the reduction of their aspect ratio. As was successfully demonstrated experimentally, for lower CNT contents the de-agglomeration mechanism may be favored against breakage via the application of "softer" dispersion protocols, which, in this study involved the application of lower amplitude ultrasound with increased sonication times while keeping the energy input in the system constant. More analytically, in the case of the 0.5 % CNT loading the increase in fracture toughness was spectacular reaching almost 400 % compared to the initial sonication protocol and almost 600 % compared to the neat epoxy system. The 1.0 % CNT nanocomposite exhibited significant but much less spectacular enhancement, with 50 % enhancement compared to the initial sonication protocol and 130 % enhancement compared to the neat epoxy. The discrepancy between the two studied systems was attributed to the increasing difficulty to disperse the nano-reinforcement with increasing content, which potentially sets a limit to the maximum CNT loading that may be efficiently dispersed in the nanocomposite matrix.

The adoption of a simple geometrical analogue which describes both dominant mechanisms that take place during dispersion, allowed for the analytical modelling of the dispersion process via the application of well-known models that describe the equivalent composite properties for stiffness, strength and finally fracture toughness. The modified Halpin–Tsai model was successful in depicting the antagonistic effect of deagglomeration and breakage, both for stiffness and strength, but the calculated strength values were underestimated for both studied CNT contents. The calculated toughness values were in very good agreement with the experimentally obtained values. As was shown, in the case of the 0.5 % CNT content, the corresponding calculated values indicated that the reinforcement efficiency of the initial dispersion protocol could be substantially optimised via the tailoring of the dispersion process in order to favour the de-agglomeration mechanism, which was successfully performed in the optimized protocol. In the latter case, the attained values were found to reach approximately

80 % of the theoretically maximum reinforcement efficiency. In the case of 1.0 % reinforcement, the initial protocol was found to be totally unsuccessful in efficiently dispersing the CNTs in the matrix, as the experimentally measured toughness value barely reached the minimum calculated value. The application of the optimised protocol, indicated that even in the case of 1.0 %, de-agglomeration may be favoured to breakage, but, as was observed experimentally the attained toughness values are far from optimal, suggesting again that higher CNT loading poses a limit to the efficient dispersion potential of the system.

References

1. Kinloch AJ et al (1983) Deformation and fracture behaviour of a rubber-toughened epoxy: 1. Microstructure and fracture studies. Polymer 24(10):1341–1354
2. Yee AF, Pearson RA (1986) Toughening mechanisms in elastomer-modified epoxies. J Mater Sci 21(7):2462–2474
3. Kinloch AJ (2003) Toughening epoxy adhesives to meet today's challenges. MRS Bull 28(6):445–448
4. Hourston DJ, Lane JM (1992) The toughening of epoxy resins with thermoplastics: 1. trifunctional epoxy resin–polyetherimide blends. Polymer 33(7):1379–1383
5. Lee J, Yee AF (2000) Fracture of glass bead/epoxy composites: on micro-mechanical deformations. Polymer 41(23):8363–8373
6. Hsieh TH et al (2010) The mechanisms and mechanics of the toughening of epoxy polymers modified with silica nanoparticles. Polymer 51(26):6284–6294
7. Dittanet P, Pearson RA (2012) Effect of silica nanoparticle size on toughening mechanisms of filled epoxy. Polymer 53(9):1890–1905
8. Minopoulou E et al (2003) Use of NIR for structural characterization of urea-formaldehyde resins. Int J Adhes Adhes 23(6):473–484
9. Subramaniyan AK, Sun CT (2007) Toughening polymeric composites using nanoclay: crack tip scale effects on fracture toughness. Compos A 38(1):34–43
10. Quaresimin M, Salviato M, Zappalorto M (2012) Fracture and interlaminar properties of clay-modified epoxies and their glass reinforced laminates. Eng Fract Mech 81:80–93
11. Silani M et al (2012) On the experimental and numerical investigation of clay/epoxy nanocomposites. Compos Struct 94(11):3142–3148
12. Bai JB, Allaoui A (2003) Effect of the length and the aggregate size of MWNTs on the improvement efficiency of the mechanical and electrical properties of nanocomposites—experimental investigation. Compos A 34(8):689–694
13. Gkikas G, Barkoula NM, Paipetis AS (2012) Effect of dispersion conditions on the thermo-mechanical and toughness properties of multi walled carbon nanotubes-reinforced epoxy. Compos B 43(6):2697–2705
14. Shaffer M, Kinloch IA (2004) Prospects for nanotube and nanofibre composites. Compos Sci Technol 64(15):2281–2282
15. Mirjalili V, Hubert P (2010) Modelling of the carbon nanotube bridging effect on the toughening of polymers and experimental verification. Compos Sci Technol 70(10):1537–1543
16. Tang L-C et al (2013) Fracture toughness and electrical conductivity of epoxy composites filled with carbon nanotubes and spherical particles. Compos A 45:95–101
17. Spitalsky Z et al (2010) Carbon nanotube–polymer composites: chemistry, processing, mechanical and electrical properties. Prog Polym Sci 35(3):357–401
18. Bortz DR, Merino C, Martin-Gullon I (2011) Carbon nanofibers enhance the fracture toughness and fatigue performance of a structural epoxy system. Compos Sci Technol 71(1):31–38
19. Patton RD et al (1999) Vapor grown carbon fiber composites with epoxy and poly(phenylene sulfide) matrices. Compos A 30(9):1081–1091
20. Rafiee MA et al (2010) Fracture and fatigue in graphene nanocomposites. Small 6(2):179–183
21. Young RJ et al (2012) The mechanics of graphene nanocomposites: a review. Compos Sci Technol 72(12):1459–1476
22. Iijima S (1991) Helical microtubules of graphitic carbon. Nature 354(6348):56–58
23. Grammatikos SA, Gkikas G, Paipetis A (2011) Monitoring strain and damage in multi-phase composite materials using electrical resistance methods. Proc SPIE 7982:79820K
24. Ueda M, Todoroki A (2006) Asymmetrical dual charge EPCM for delamination monitoring of CFRP laminate. Key Eng Mater 321–323:1309–1315
25. Gkikas G et al (2012) Enhanced bonded aircraft repair using nano-modified adhesives. Mater Des 41:394–402
26. Bertolini Cestari C et al (2013) The reinforcement of ancient timber-joints with carbon nano-composites. Meccanica 48(8):1925–1935
27. Barkoula NM et al (2009) Environmental degradation of carbon nanotube-modified composite laminates: a study of electrical resistivity. Mech Compos Mater 45(1):21–32
28. Grammatikos SA et al (2012) Low-velocity impact damage identification using a novel current injection thermographic technique. Proceedings of SPIE—The International Society for Optical Engineering 8346
29. Karapappas P et al (2009) Enhanced fracture properties of carbon reinforced composites by the addition of multi-wall carbon nanotubes. J Compos Mater 43(9):977–985
30. Kostopoulos V et al (2010) Impact and after-impact properties of carbon fibre reinforced composites enhanced with multi-wall carbon nanotubes. Compos Sci Technol 70(4):553–563
31. Kostopoulos V et al (2011) Interlaminar fracture toughness of carbon fibre-reinforced polymer laminates with nano- and micro-fillers. Strain 47(SUPPL. 1):e269–e282
32. Vavouliotis A et al (2009) Multistage fatigue life monitoring on carbon fibre reinforced polymers enhanced with multiwall carbon nanotubes. Plast Rubber Compos 38(2–4):124–130
33. Vavouliotis A, Paipetis A, Kostopoulos V (2011) On the fatigue life prediction of CFRP laminates using the

electrical resistance change method. Compos Sci Technol 71(5):630–642
34. Grammatikos SA et al (2014) Current injection phase thermography for low-velocity impact damage identification in composite laminates. Mater Des 55:429–441
35. Grammatikos SA et al (2013) Real-time debonding monitoring of composite repaired materials via electrical, acoustic, and thermographic methods. J Mater Eng Perform 1–12
36. Paipetis AS, Kostopoulos V (2013) Carbon nanotubes for novel hybrid structural composites with enhanced damage tolerance and self-sensing/actuating abilities. Springer, Dordrecht, pp 1–20
37. Xie S et al (2000) Mechanical and physical properties on carbon nanotube. J Phys Chem Solids 61(7):1153–1158
38. Wong M et al (2003) Physical interactions at carbon nanotube–polymer interface. Polymer 44(25):7757–7764
39. Boura O et al (2013) Carbon nanotube growth on high modulus carbon fibres: morphological and interfacial characterization. Surf Interface Anal 45(9):1372–1381
40. Fidelus JD et al (2005) Thermo-mechanical properties of randomly oriented carbon/epoxy nanocomposites. Compos A 36(11):1555–1561
41. Chakraborty A et al (2011) Carbon nanotube (CNT)–epoxy nanocomposites: a systematic investigation of CNT dispersion. J Nanopart Res 13(12):6493–6506
42. Rachmadini Y, Tan VBC, Tay TE (2010) Enhancement of mechanical properties of composites through incorporation of CNT in VARTM: a review. J Reinf Plast Compos 29(18):2782–2807
43. Yeh M-K, Hsieh T-H, Tai N-H (2008) Fabrication and mechanical properties of multi-walled carbon nanotubes/epoxy nanocomposites. Mater Sci Eng A 483–484:289–292
44. Seyhan AT, Tanoğlu M, Schulte K (2009) Tensile mechanical behavior and fracture toughness of MWCNT and DWCNT modified vinyl-ester/polyester hybrid nanocomposites produced by 3-roll milling. Mater Sci Eng A 523(1–2):85–92
45. Lee JH, Rhee KY, Park SJ (2010) The tensile and thermal properties of modified CNT-reinforced basalt/epoxy composites. Mater Sci Eng A 527(26):6838–6843
46. Gojny FH et al (2004) Carbon nanotube-reinforced epoxy-composites: enhanced stiffness and fracture toughness at low nanotube content. Compos Sci Technol 64(15):2363–2371
47. Rafiee MA et al (2009) Enhanced Mechanical Properties of Nanocomposites at Low Graphene Content. ACS Nano 3(12):3884–3890
48. Zhang W et al (2009) Heterogeneity in epoxy nanocomposites initiates crazing: significant improvements in fatigue resistance and toughening. Small 5(12):1403–1407
49. Brcic M, Canadija M, Brnic J (2013) Estimation of material properties of nanocomposite structures. Meccanica 48(9):2209–2220
50. Blanco J et al (2009) Limiting mechanisms of mode I interlaminar toughening of composites reinforced with aligned carbon nanotubes. J Compos Mater 43(8):825–841
51. Wicks SS, de Villoria RG, Wardle BL (2010) Interlaminar and intralaminar reinforcement of composite laminates with aligned carbon nanotubes. Compos Sci Technol 70(1):20–28
52. Gkikas G, Douka DD, Barkoula NM, Paipetis AS (2013) Interlaminar shear strength and thermo-mechanical properties of nano-enhanced composite materials under thermal shock. Proc SPIE 8689:86891Q
53. Mukhopadhyay K, Dwivedi CD, Mathur GN (2002) Conversion of carbon nanotubes to carbon nanofibers by sonication. Carbon 40(8):1373–1376
54. Miyagawa H, Drzal LT (2004) Thermo-physical and impact properties of epoxy nanocomposites reinforced by single-wall carbon nanotubes. Polymer 45(15):5163–5170
55. Kostopoulos V et al (2007) Mode I interlaminar fracture of CNF or/and PZT doped CFRPs via acoustic emission monitoring. Compos Sci Technol 67(5):822–828
56. Darweschsad M et al (1997) Development and test of the poloidal field prototype coil POLO at the Forschungszentrum Karlsruhe. Fusion Eng Des 36(2–3):227–250
57. Rosato D (2003) Glossary. Plastics engineered product design. Elsevier Science, Amsterdam, pp 493–546
58. So HH, Cho JW, Sahoo NG (2007) Effect of carbon nanotubes on mechanical and electrical properties of polyimide/carbon nanotubes nanocomposites. Eur Polym J 43(9):3750–3756
59. Nadler M et al (2009) Effect of CNT surface functionalisation on the mechanical properties of multi-walled carbon nanotube/epoxy-composites. Compos A 40(6–7):932–937
60. Gojny FH et al (2005) Influence of different carbon nanotubes on the mechanical properties of epoxy matrix composites: a comparative study. Compos Sci Technol 65(15–16):2300–2313
61. Montazeri A et al (2011) An investigation on the effect of sonication time and dispersing medium on the mechanical properties of MWCNT/epoxy nanocomposites. Adv Mater 264–265:1954–1959
62. Watson AS, Smith RL (1985) An examination of statistical theories for fibrous materials in the light of experimental data. J Mater Sci 20(9):3260–3270
63. Aggelis DG, Soulioti D, Barkoula NM, Paipetis AS, Matikas TE, Shiotani T (2009) Acoustic emission of steel-fiber concrete under four-point bending. Proc SPIE 7294:729407
64. Kostopoulos V et al (2009) Damage monitoring of carbon fiber reinforced laminates using resistance measurements. Improving sensitivity using carbon nanotube doped epoxy matrix system. J Intell Mater Syst Struct 20(9):1025–1034
65. Shaffer MSP, Fan X, Windle AH (1998) Dispersion and packing of carbon nanotubes. Carbon 36(11):1603–1612
66. Yeh M-K, Tai N-H, Liu J-H (2006) Mechanical behavior of phenolic-based composites reinforced with multi-walled carbon nanotubes. Carbon 44(1):1–9
67. Affdl JCH, Kardos JL (1976) The Halpin–Tsai equations: a review. Polym Eng Sci 16(5):344–352
68. Fisher FT, Bradshaw RD, Brinson LC (2003) Fiber waviness in nanotube-reinforced polymer composites—I: modulus predictions using effective nanotube properties. Compos Sci Technol 63(11):1689–1703
69. Shao LH et al (2009) Prediction of effective moduli of carbon nanotube–reinforced composites with waviness and debonding. Compos Struct 87(3):274–281
70. Shady E, Gowayed Y (2010) Effect of nanotube geometry on the elastic properties of nanocomposites. Compos Sci Technol 70(10):1476–1481
71. Cox HL (1952) The elasticity and strength of paper and other fibrous materials. Br J Appl Phys 3(3):72–79

72. Hsieh TH et al (2011) The effect of carbon nanotubes on the fracture toughness and fatigue performance of a thermosetting epoxy polymer. J Mater Sci 46(23):7525–7535
73. Yu M-F et al (2000) Strength and breaking mechanism of multiwalled carbon nanotubes under tensile load. Science 287(5453):637–640
74. Xie X-L, Mai Y-W, Zhou X-P (2005) Dispersion and alignment of carbon nanotubes in polymer matrix: a review. Mater Sci Eng R 49(4):89–112
75. Tai N-H, Yeh M-K, Peng T-H (2008) Experimental study and theoretical analysis on the mechanical properties of SWNTs/phenolic composites. Compos B 39(6):926–932
76. Hull D, Clyne TW (1996) An introduction to composite materials, 2nd edn. Cambridge University Press, Cambridge
77. Yu MF et al (2000) Strength and breaking mechanism of multiwalled carbon nanotubes under tensile load. Science 287(5453):637–640
78. Demczyk BG et al (2002) Direct mechanical measurement of the tensile strength and elastic modulus of multiwalled carbon nanotubes. Mater Sci Eng A 334(1–2):173–178
79. Kim J-K, Mai Y-W (1998) Engineered interfaces in fiber reinforced composites. Elsevier Science Ltd, Oxford
80. Wichmann MHG, Schulte K, Wagner HD (2008) On nanocomposite toughness. Compos Sci Technol 68(1):329–331
81. Tsantzalis S et al (2007) On the improvement of toughness of CFRPs with resin doped with CNF and PZT particles. Compos A 38(4):1159–1162
82. Fiedler B et al (2006) Fundamental aspects of nano-reinforced composites. Compos Sci Technol 66(16):3115–3125
83. Barber AH, Cohen SR, Wagner HD (2003) Measurement of carbon nanotube–polymer interfacial strength. Appl Phys Lett 82(23):4140–4142
84. Barber AH et al (2004) Interfacial fracture energy measurements for multi-walled carbon nanotubes pulled from a polymer matrix. Compos Sci Technol 64(15):2283–2289
85. Huang Y, Kinloch AJ (1992) Modelling of the toughening mechanisms in rubber-modified epoxy polymers. J Mater Sci 27(10):2753–2762
86. Sultan JN, McGarry FJ (1973) Effect of rubber particle size on deformation mechanisms in glassy epoxy. Polym Eng Sci 13(1):29–34
87. Guild FJ, Young RJ (1989) A predictive model for particulate-filled composite materials. J Mater Sci 24(1):298–306
88. Guild FJ, Young RJ (1989) A predictive model for particulate filled composite materials. J Mater Sci 24(7):2454–2460
89. Zhandarov S et al (2001) Investigation of load transfer between the fiber and the matrix in pull-out tests with fibers having different diameters. J Adhes Sci Technol 15(2):205–222